Nitric Oxide 93 (2019) 34–43

Contents lists available at ScienceDirect

Nitric Oxide

journal homepage: www.elsevier.com/locate/yniox

Inhibition of breast tumor growth by N(G)-nitro-L-arginine methyl ester (L-NAME) is accompanied by activation of fibroblasts

Marianela Sciacca[a], Denise Belgorosky[a], Macarena Zambrano[a], José Ignacio Gómez Escalante[b], Fernanda Roca[b], Yanina V. Langle[a], Eduardo O. Sandes[a], Catalina Lodillinsky[a,c,**,1], Ana María Eiján[a,c,*,1]

[a] Research Area, Instituto de Oncología Ángel H. Roffo, Universidad de Buenos Aires, Buenos Aires, Argentina
[b] Department of Pathology, Instituto de Oncología Ángel H. Roffo, Universidad de Buenos Aires, Buenos Aires, Argentina
[c] Member of Consejo Nacional de Investigaciones Científicas y Técnicas (CONICET), Argentina

ARTICLE INFO

Keywords:
Breast cancer
iNOS
Nitric oxide
Fibroblast

ABSTRACT

Nitric Oxide (NO) is involved in many physiological and pathological processes. It is generated by a family of NO synthases (NOS), being the inducible isoform, iNOS, responsible for higher amounts of NO. Here, we report that pharmacological inhibition of NO production by L-NAME reduces both viability and MAPK activated signalling pathways in iNOS positive human and murine cancer cell lines. In vivo, using syngeneic models, in parallel with tumor reduction induced by L-NAME, collagen deposition and α-SMA positive stromal cells are observed. This observation takes place only when tumor cells express iNOS. In vitro, L-NAME induces viability and differentiation on fibroblast. Our results reveal that NO inhibition contributes to stimulate proliferation and activation of fibroblasts in parallel with tumor reduction of iNOS positive breast cancer.

1. Introduction

Breast cancer is the most common type of cancer in women in the entire world. In Argentina, breast cancer is the one with the highest death incidence, also. More than 19,300 new cases per year have been estimated and 6,000 deaths show that breast cancer research is very relevant worldwide and locally [1].

About 70% of breast cancers are sensitive to estrogen or progesterone hormones. Due to that, this type of cancer is treated with antagonists such as tamoxifen or aromatase inhibitors. Among tumors that are negative for hormone receptors, we can find the positive HER2 and the triple negative (TNBC) (negative for hormone receptors and HER2) subtypes [2]. Chemotherapy combined with anti-HER2 therapy may be of benefit for patients whose tumor belongs to the HER2 subtype. Unfortunately, there is no additional treatment for TNBC subtypes. Therefore, the identification of new therapeutic targets is essential in this oncological pathology.

Nitric Oxide (NO) is a free radical signaling molecule, involved in different biological processes. NO is produced by nitric oxide synthases. Two of them that are constitutively expressed (neuronal, nNOS and endothelial, eNOS) produce nano molar NO levels. On the other hand, the inducible isoform (iNOS) produces higher NO levels, in a micro molar order [3]. This intracellular second messenger can promote either cell death or cell survival depending on cell type. Low concentrations of NO participate in physiological processes involving cGMP, such as neurotransmission and vascular dilatation. However, high concentrations of NO show results that are more controversial. They can modify cell signaling at different levels, such as oxidation of sphingolipids, inactivation of metal-dependent enzymes, mutations in p53 and/or damage in the DNA among others [040].

In tumor biology, NO also has a controversial role. There is evidence that NO can both inhibit and stimulate tumor cell growth [5]. This response depends on tumor type, genetic background, NO levels and sensibility in the target cells [6]. Most of NO biological effects are mediated through modulation of signaling pathways. Tumor progression was linked to the NO ability to induce EGFR-dependent ERK phosphorylation, that promotes cell migration and invasion [7].

Correlation between iNOS expression and clinical outcome associated to worse prognosis, was evaluated in breast, bladder, gastric and oral squamous cell carcinoma, among other types of tumors [7–9].

* Corresponding author. Research Area, Instituto de Oncología Ángel H. Roffo, Universidad de Buenos Aires, Buenos Aires, Argentina.;
** Corresponding author. Instituto de Oncología Ángel H. Roffo, Universidad de Buenos Aires, Av. San Martín 5481, CP 1417, DTB Buenos Aires, Argentina.
E-mail addresses: clodillinsky@institutoroffo.uba.ar (C. Lodillinsky), anamariaeijan@gmail.com, grupoeijan@gmail.com (A.M. Eiján).
[1] These authors shared the project management.

https://doi.org/10.1016/j.niox.2019.09.008
Received 2 November 2018; Received in revised form 17 September 2019; Accepted 18 September 2019
Available online 19 September 2019
1089-8603/

Inhibition of iNOS has been proposed as a targeted therapy in several types of tumors, including breast cancer [10,11]. Moreover, in TNBC, iNOS expression was correlated with aggressiveness, poor survival, and treatment resistance [11–14].

The functionality of NO as a proangiogenic factor is well characterized [15]. In a tumoral microenvironment, not only are vasculature cells associated with NO modulation, inflammatory cells such as macrophages and neutrophils carry out their role through the induction of the expression of iNOS and consequently through NO production [16,17]. Fibroblast, the cell type that synthetizes the extracellular matrix, mainly collagen, has been linked to tumor progression. Activated fibroblasts secrete and activate several growth factors and are responsible for cancer associated desmoplasia [18]. Their role in cancer depends on tumor type. Even though collagen deposition is often associated with tumor progression [19], sometimes it does not seem to be the case [20–22]. The role of fibroblasts in breast cancer associated to NO inhibition has not been yet elucidated.

In this work, we use murine and human breast cancer cell lines to evaluate the impact of NO inhibition in tumor progression. LM3 a cell line, derived from a murine mammary adenocarcinoma and LMM3, a more aggressive variant that express iNOS, as well as the human MDA-MB-231 cells, and, murine LM2 and human MCF10DCIS.com, with negligible levels of enzyme are included. We focus on both, tumor and fibroblast as NO-inhibition-target cells during tumor growth rate decline. Our findings indicate that L-NAME, a competitive inhibitor for iNOS, induces tumor growth reduction only when cancer cells express iNOS. When this is the case, activation and differentiation of fibroblast are observed concurrently. Our findings suggest that inhibition of NO production does not only offer a benefit by blocking tumor cell growth but also by activating components of the stroma such as fibroblasts.

2. Results

L-NAME inhibits in vitro proliferation and MAPK signaling pathway activation.

With the aim of analyzing NOS status and its own product in breast cancer cells, we evaluated the expression of the enzyme and nitrite production. The mouse mammary tumor cells line, LM3 and its more aggressive variant LMM3 expressed iNOS at basal levels that were not modified under the nitric oxide inhibitor, L-NAME, treatment. On the other hand, LM2, another mouse mammary tumor cell line did not express iNOS (Fig. 1A). iNOS mRNA was also evaluated. LM3 and LMM3 present higher levels of iNOS mRNA compared to LM2. We observed higher levels of iNOS mRNA in LMM3 compared to LM3 and no difference was observed in cells treated with L-NAME (Fig. 1B). Moreover, none of the three cell lines expressed neither nNOS nor eNOS (Fig. 1A). Consistent with iNOS expression, both LM3 and LMM3 produced NO, which was reduced by L-NAME (Fig. 1C).

When cell viability was evaluated, NO inhibition on iNOS-positive cells induced a reduction in cell viability. Different from what we observed on LM3 and LMM3, the iNOS-negative cell line, LM2, did not produce NO and its viability was not affected under L-NAME treatment (Fig. 1C and D). To analyze the impact of NO over the cells, we tested the viability after treatment with DETA/NO, a NO donor. DETA/NO induced cell viability in both, LM3 and LMM3, but not in LM2 cells, indicating that LM3 and LMM3 expressing iNOS, produced NO and were affected to it at 60 and 125 μM (Fig. 1E). Higher concentration, such as 250 μM of DETA/NO did not increase cell viability, suggesting that higher levels of NO may affect negatively in the cell proliferation machinery.

Since it is known that NO is involved in ERK phosphorylation, we wonder if L-NAME treatment could modify this activation. A serum starvation experiment was made. LM3, LMM3 and LM2 monolayers were treated overnight with 2 mM of L-NAME in absence of serum. Then, cells were stimulated for 5, 10 and 20 min with serum, with or without L-NAME, whole-cell lysates were prepared, and immunoblotting was performed. Our results showed that serum induced ERK phosphorylation at 5 and 10 min for LM3 and LMM3. This effect was inhibited when the cells were treated with L-NAME (Fig. 2A–D). Interestingly, L-NAME was able to block serum-induced ERK phosphorylation only in iNOS positive cells, LM3 and LMM3. In contrast, in iNOS negative cell line, LM2, serum induced ERK phosphorylation even though L-NAME was not able to reverse this effect (Fig. 2E and F).

With the idea of extending these findings, human cells were also analyzed. We evaluated iNOS expression in two different breast cancer cell lines. MDA-MB-231 expressed higher levels of the enzyme compared to MCF10DCIS.com cells (Fig. 3A). Like what we observed in murine iNOS positive cells, NO inhibition by L-NAME reduced and DETA/NO induced cell viability in MDA-MB-231 cells, but none of them affected cell viability in MCF10DCIS.com cells (Fig. 3B). In the same line, L-NAME blocked serum-induced ERK phosphorylation in MDA-MB-231 (Fig. 3C and D) but was not able to reverse this effect in MCF10DCIS.com cell line (Fig. 3E and F).

These results indicate that inhibition of MAPK signaling pathway is, at least in part, one of the mechanisms involved during tumor cell proliferation blockade by L-NAME and that endogenous NO production may contribute to serum-induced MAPK molecular pathway in iNOS positive cells.

2.1. L-NAME inhibits iNOS positive tumor growth

To analyze the effect of NO inhibition in breast cancer progression, the three murine cell lines were injected in the fat pad tissue of BALB/c females. Mice were then randomized into two groups and one of them received L-NAME in the drinking water. Analysis of tumor volume in both LM3 and LMM3 tumors revealed, significantly smaller tumors arising from L-NAME treated mice compared to control (CRL) group (Fig. 4A). Interestingly, no difference was observed in M2 tumors. Thus, only iNOS expressing cells such as LM3 and LMM3 were able to respond to L-NAME, while iNOS negative LM2 cell line did not show differences in tumor growth.

Histopathological studies revealed that LM3 and LMM3 cells fat pad inoculation fostered the development of epithelial tumors, where cells were compactly arranged in a syncytial sheet manner, without a defined pattern (Fig. 4B c and f). Large necrotic area (Fig. 4B a and d) and inflammatory infiltrate were observed (Fig. 4B b and e). Tumors treated with L-NAME were characterized by the presence of more scattered cells. In some sectors the neoplastic cells formed nests and cords delimited by connective tissue (Fig. 4B l and o). LM2 tumors were also characterized by compactly arranged cells with less necrotic area and inflammatory infiltration compared to LM3 or LMM3 ones (Fig. 4B i, g and h respectively). In this case, no difference was observed when tumors received L-NAME (Fig. 4B p, q and r).

iNOS expression was tested in tumors growing in fat pad. We observed that LM3 and LMM3 tumors were positive for iNOS. No significant changes were observed under L-NAME treatment. Consistent with the result observed in vitro, LM2 tumors were negative for the enzyme (Fig. 4C).

2.2. L-NAME induce collagen deposition in breast tumors

Changes in stroma remodeling induced by L-NAME in bladder cancer have already been described [21]. In order to analyze collagen deposition associated to tumor growth inhibition by NO blockade in breast cancer in vivo models, we performed a Trichrome Masson staining of LM3, LMM3 and LM2 tumor sections from tumor-bearing mice under or not L-NAME treatment. In LM3 and LMM3 tumors receiving L-NAME, cruciform and stellated shaped collagen positive cells compatible with activated fibroblast were observed. Globally, our results showed that L-NAME was able to induce a stroma reaction with collagen deposition only in iNOS positive tumors (Fig. 5A). In order to

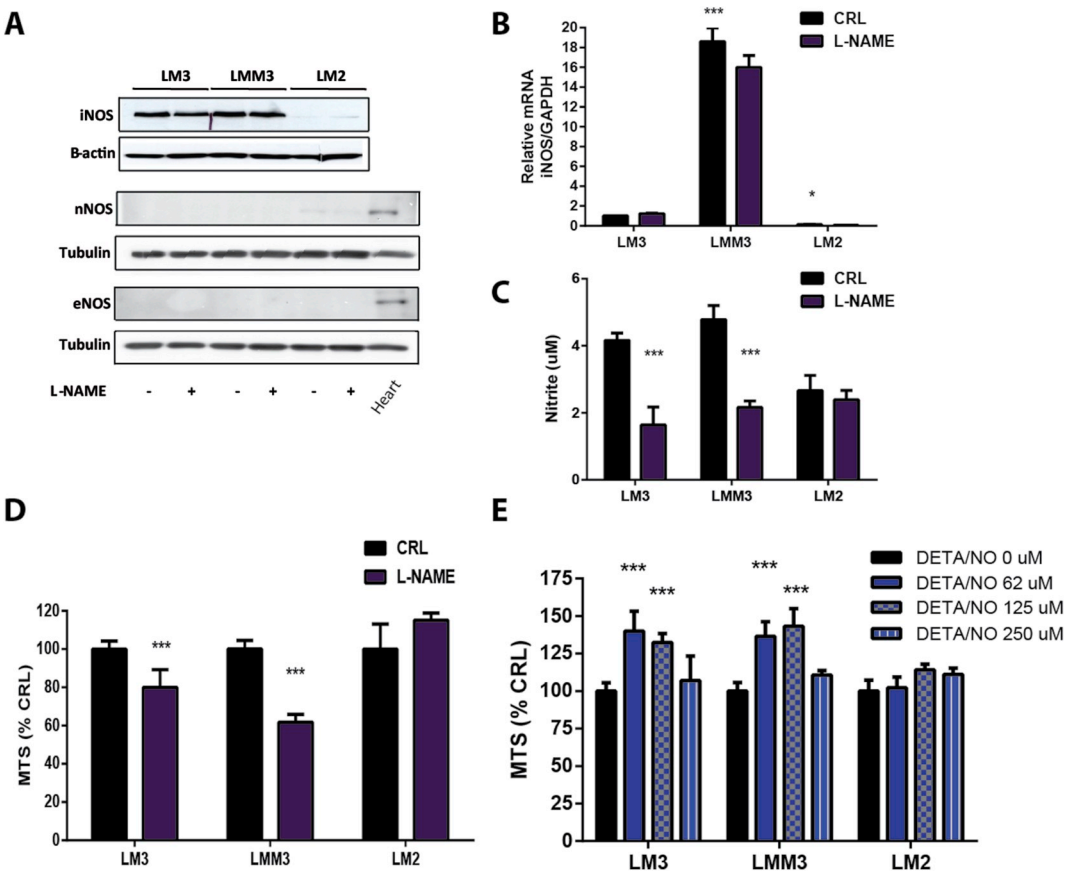

Fig. 1. Effect of NO on tumor breast murine cells. (A) Expression of NOS isoforms were determined in LM3, LMM3 and LM2 mouse breast cancer cells by Western Blot in presence or absence of L-NAME and B-actin or Tubulin was used as a loading control. Mouse heart lysate was used as a positive control. (B) RT-qPCR for iNOS mRNA expression level in cells treated or not with L-NAME. Values are means ± SEM, n = 3 independent experiments of relative amounts of amplified iNOS mRNA normalized against GAPDH. *p < 0.05; ***p < 0,001 by two-way ANOVA, Bonferroni post-test vs LM3. No statistical difference was found between CRL vs L-NAME. (C) NO production was determined in the supernatants of three cell lines by Griess reagent in presence or absence of L-NAME (2 mM) for 24 h. ***p < 0.001 vs CRL. (D) Cells were treated with L-NAME (2 mM) for 48 h, cell viability was evaluated by MTS. (E) Cells were treated with DETA/NO (62, 125 and 250 μM) for 24 h and cell viability was evaluated by MTS. ***p < 0.001 by two-way ANOVA, Bonferroni post-test vs CRL.

further analyze stroma remodeling, Picrosirious Red, another fibrillar collagen staining was also performed in paraffin sections. Our results showed that collagen fibers deposition was significatively increased in LM3 and LMM3 tumors from mice treated with L-NAME compared to CRL (Fig. 5B and C). No difference was observed in LM2 tumors. Since fibroblasts are the main collagen source, all together, this result indicates that NO produced by tumor cells could act as a negative regulator of fibroblast activation in breast cancer.

2.3. L-NAME induces fibroblast activation

Concurrently while tumor growth declined, our results showed that NO inhibition induced collagen fibers deposition. To analyze whether L-NAME was able to induce fibroblast activation, NIH-3T3 cells were treated with L-NAME 2 mM and viability (MTS) and activation (Smooth Muscle Actin-α -αSMA-expression) were analyzed. We observed that viability of cells under L-NAME treatment was higher compared to CRL condition. In contrast, treatment with the NO-donor, DETA/NO, reduced viability on the fibroblasts (Fig. 6A). Furthermore, we could observe that α-SMA expression was increased when cells received L-NAME (Fig. 6B), indicating that besides cell viability, NO inhibition induced cell differentiation.

Since L-NAME abolished serum-induced ERK activation in tumor cells (Fig. 2A and C), we wondered whether fibroblast could respond to serum stimulus and L-NAME treatment. NIH-3T3 monolayer was treated overnight with L-NAME (2 mM) in absence of serum. Then, cells were stimulated for 5, 10 and 20 min with serum, with or without L-NAME, whole-cell lysates were prepared, and immunoblotting was performed. We observed that serum induced ERK phosphorylation at 5 min. Contrary to iNOS positive tumor cells, L-NAME did not modulate this induction on fibroblast (Fig. 6C and D). All together data indicate that NO inhibition induced viability and activation of fibroblast without affecting MAPK signaling pathway.

Finally, α-SMA expression was also analyzed in vivo. Concomitant to what we observed in vitro; L-NAME treated tumors showed an important phenotype of activated fibroblast in iNOS positive tumors (Fig. 6E).

3. Discussion

Adjuvant treatment for breast cancer has improved patient's survival [23]. Nevertheless, it is the first cause of death in women, worldwide [24]. Hormone receptor negative-tumor patients have fewer treatment options, which highlights the need to contribute with new therapeutic targets to improve clinical parameters.

Tumors are complex entities formed by cancer cells in a continuous dialogue with tumoral microenvironment [18]. Endothelial, immune, adipocytes and fibroblast cells are-either by direct interaction or through soluble factors-intimately related during initiation and tumor progression [21].

Nitric oxide is a free radical with a fundamental role as a biological messenger. It is produced as an enzymatic product from NOS enzymes,

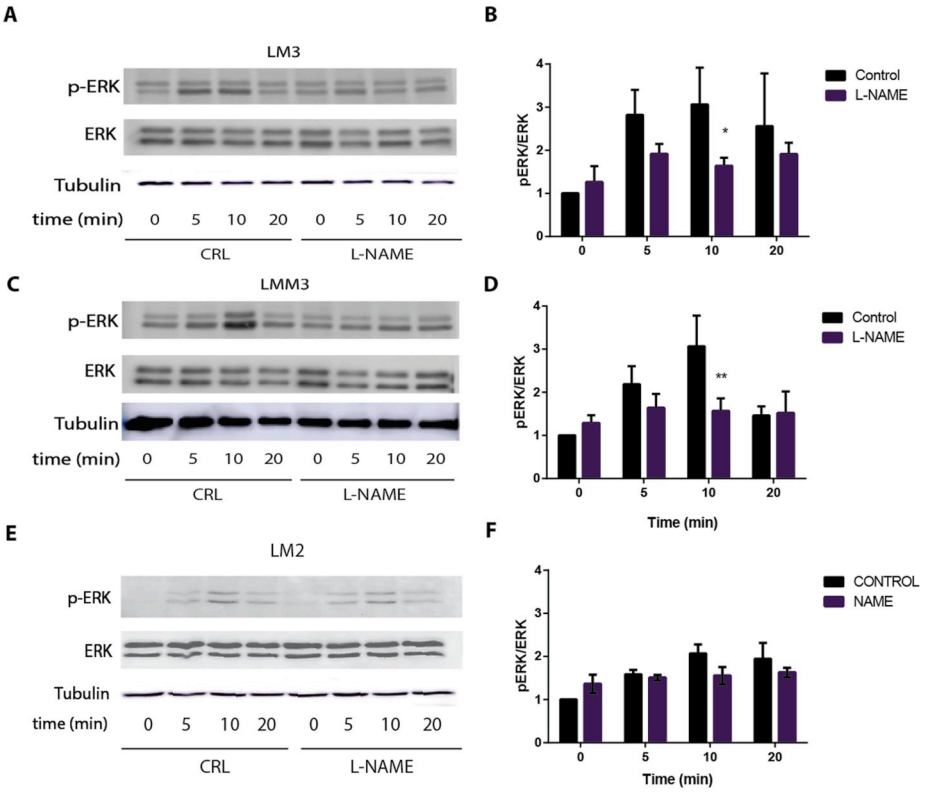

Fig. 2. Role of L-NAME on serum induced ERK activation in murine cells. Representative Western blot images of p-ERK and total ERK on (A) LM3 (C) LMM3 and (E) LM2 cells. LM3, LMM3 and LM2 monolayers were treated overnight with 2 mM of L-NAME in absence of serum. Then, cells were stimulated for 5, 10 and 20 min with serum, without (CRL) or with L-NAME. Tubulin was used as a loading control. Values are means ± SEM, n = 3 independent experiment. Relative ERK-phosphorylation levels were normalized to total protein and referred as a fold change of control (B, D and F). *p < 0.05; **P < 0.01 by two-way ANOVA, Bonferroni post-test vs Control 10 min.

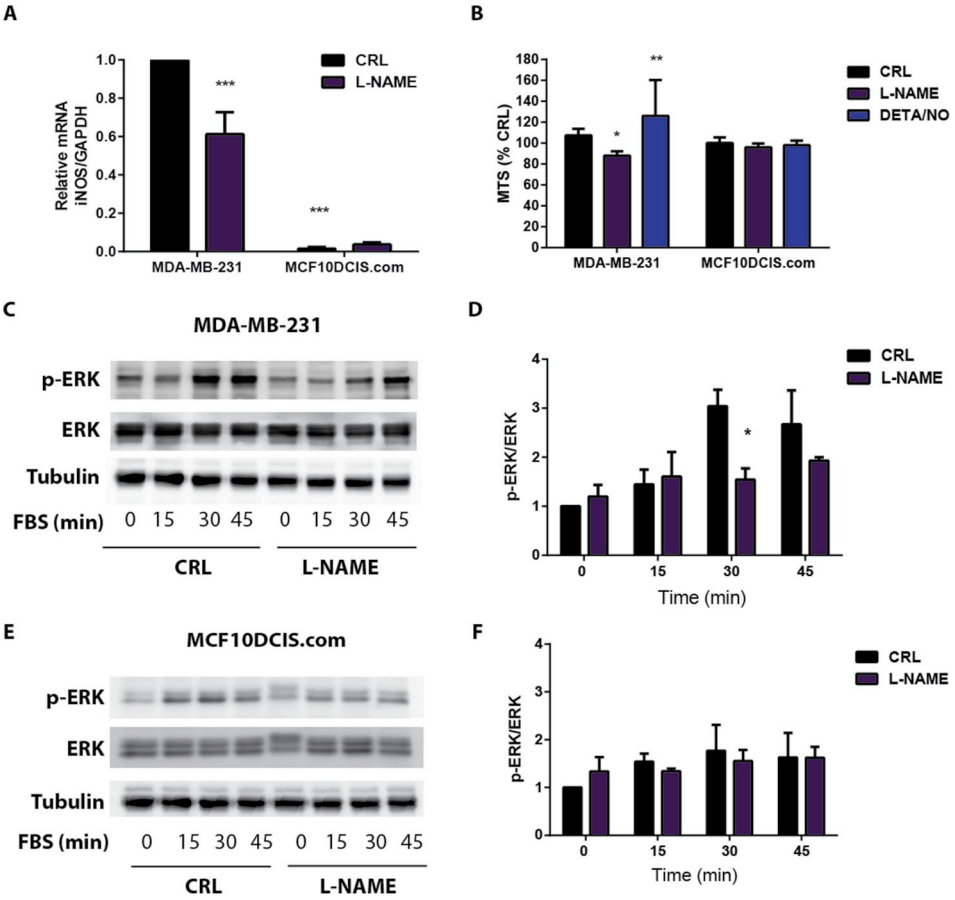

Fig. 3. Effect of 1-NAME on tumor human cell viability. (A) RT-qPCR for iNOS mRNA expression level in MDA-MB-231 and MCF10DCIS.com cells treated or not with L-NAME. Values are means ± SEM, n = 3 independent experiments of relative amounts of amplified iNOS mRNA normalized against GAPDH. ***p < 0,001 by two-way ANOVA, Bonferroni post-test vs CRL MDA-MB-231. (B) Cells were treated with L-NAME (2 mM) or DETA/NO (62 μM) for 48 h and 24 h respectively. Viability was evaluated by MTS. *p < 0.05; **p < 0,01 by two-way ANOVA, Bonferroni post-test vs CRL MDA-MB-231. Human cell monolayers were treated overnight with 2 mM of L-NAME in absence of serum. Then, cells were stimulated for 15, 30 and 45 min with serum, without (CRL) or with L-NAME. Representative Western blot images of p-ERK and total ERK on (C) MDA-MB-231 and (E) MCF10DCIS.com. Tubulin was used as a loading control. Values are means ± SEM, n = 3 independent experiment. Relative ERK-phosphorylation levels were normalized to total protein and referred as a fold change of control for (D) MDA-MB-231 or (F) MCF10DCIS.com *p < 0.05 by two-way ANOVA, Bonferroni post-test vs CRL 30 min.

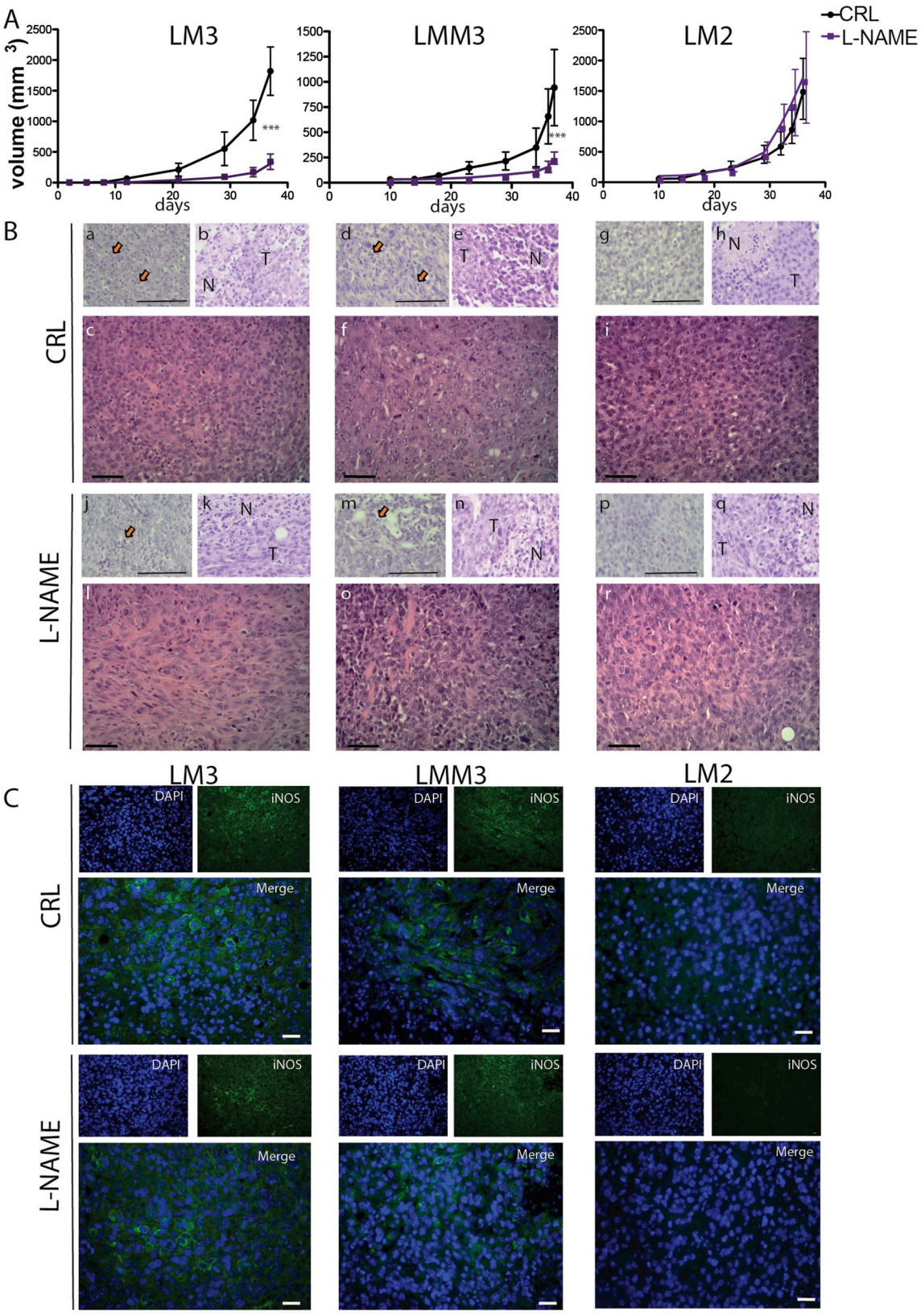

Fig. 4. In vivo assay of tumor growth under L-NAME treatment. (A) Curve of LM3, LMM3 and LM2 fat pad tumor growth. Tumors were treated with normal water (CRL) or L-NAME (0.5 g/L in drinking water). Values are means ± SD. ***p < 0.001 vs CRL by Student's t-test. (B) H&E staining of representative tumors. (a, c, g, j, m, p) H&E staining to illustrate TIL, orange arrows. (b, e, h, k, n, q) H&E stainings to illustrate necrosis area. N: necrosis; T: tumors. (c, f, i, l, o, r) H&E stainings to illustrate tumor phenotype. Scale bar: 25 μm. (C) iNOS expression in fat pad tumors (green) is illustrated in paraffin tissue section. Nuclei were stained with 4′,6-diamidino-2-phenylindole DAPI (blue). Scale bar: 5 μm.

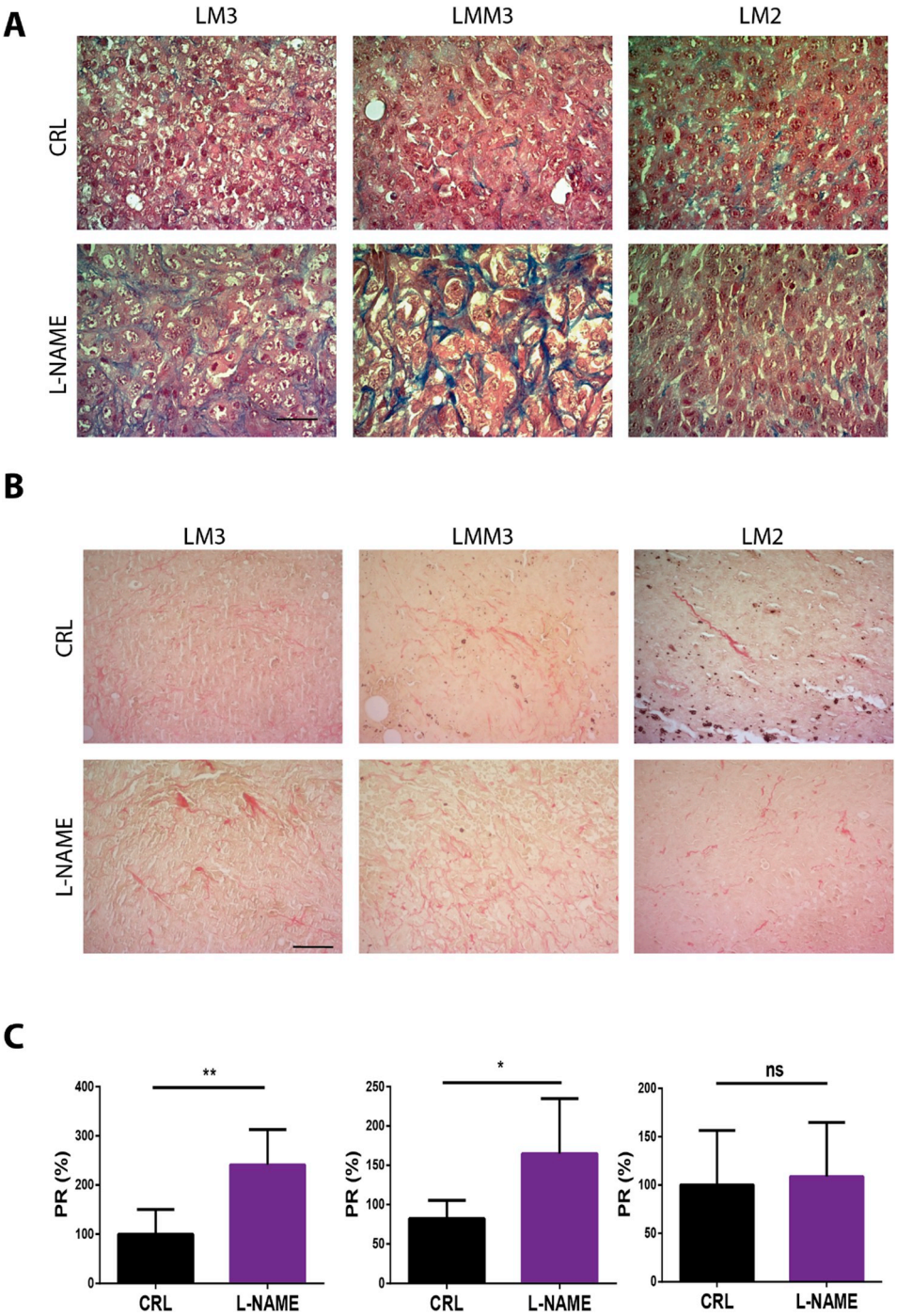

Fig. 5. In vivo collagen deposition is associated with tumor inhibition by 1-NAME. (A) Masson's Trichrome staining (collagen in blue). Scale bar: 50 μm. (B) Collagen was also analyzed by labeling with Picrosirius Red (PR) and (C) quantified (Collagen in red). *p < 0.05; **p < 0.01, L-NAME vs CRL by Student's t-test. Scale bar: 100 μm.

by several types of cells, where the inducible isoform is responsible for the production of the higher levels of this small molecule [3]. Its role in tumor biology is complex. We believe that nitric oxide carries out its protumoral activity mainly as a product from the tumor cell. To analyze this hypothesis, we used both murine and human breast cancer lines with different pattern of NOS expression. LM3 and its more aggressive variant, LMM3 as well as MDA-MB-231 expresses iNOS while LM2 and MCF10DCIS.com express low level of the enzyme. We showed here that only iNOS-positive and therefore producing NO tumor cells, were sensitive to L-NAME treatment, since it reduced cell viability and tumor growth in LM3, LMM3 and MDA-MB-231 but not in LM2 or MCF10DCIS.com cells. It has been already demonstrated that NO donor DETA/NO activates MAPK signaling pathways on tumor cells [25] and that NO stimulates tyrosine phosphorylation of proteins of the signalling pathways initiated by EGFR activation [26]. Our present results show that a NO-donor increased cell viability only in iNOS positive cells and L-NAME reduced serum-induced ERK activation only in the cell lines expressing high level of iNOS, reinforcing that in these cells, NO is acting as a survival factor.

The association between protein S-nitrosylation and protein phosphorylation has been established. [27,28]. For example, in endothelial cells, transnitrosation of p21Ras, and activation of the Ras–ERK1/2

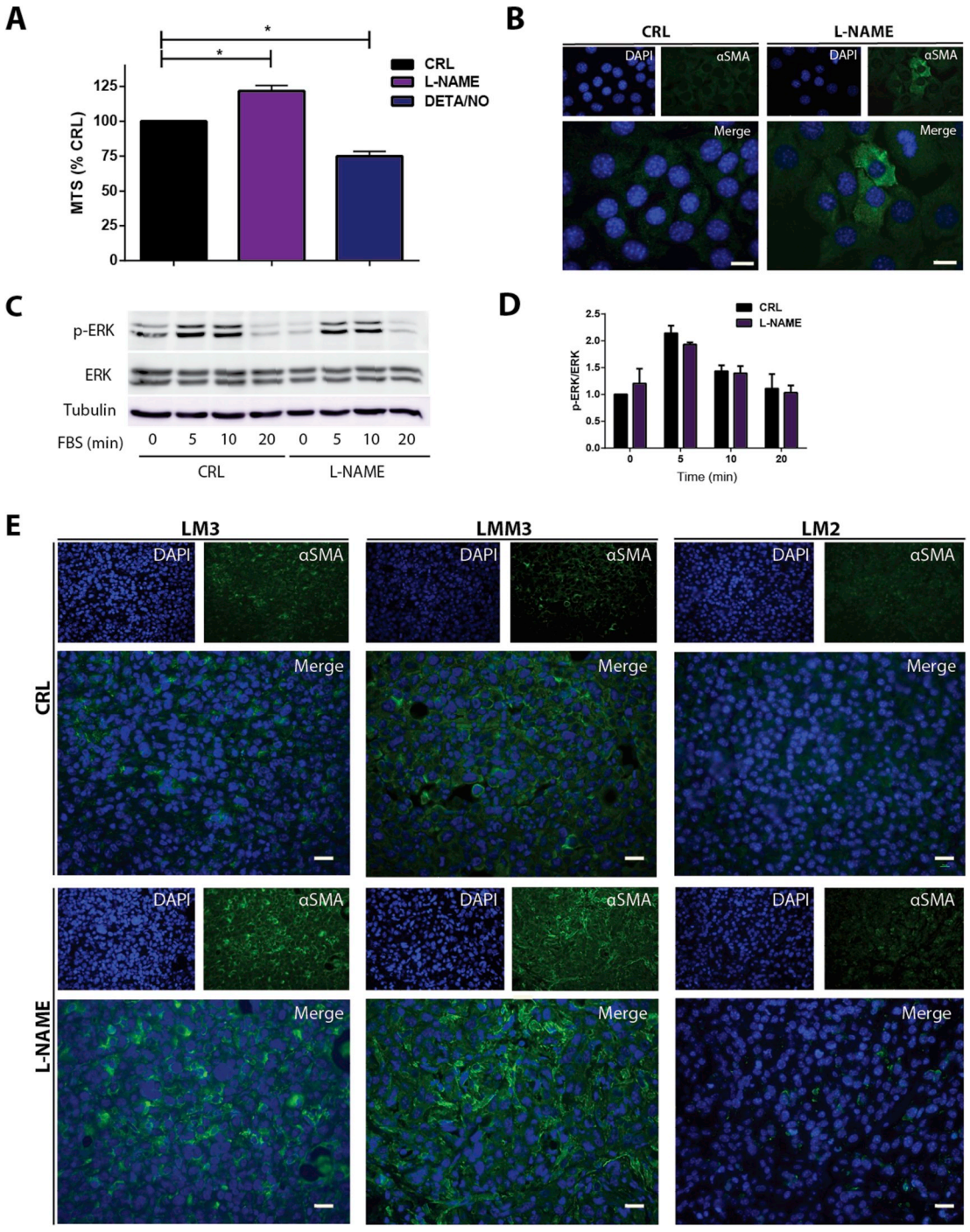

Fig. 6. Proliferation and differentiation of fibroblast under 1-NAME treatment. (A) Cells were treated with L-NAME (2 mM) or DETA/NO for 48 h and viability was evaluated by MTS. *p < 0.05 by two-way ANOVA, Bonferroni post-test vs CRL. (B) NIH-3T3 fibroblasts were treated with L-NAME 2 mM for 48 h and α-SMA (green) was analyzed by Immunofluorescence. Scale bar: 3 μm. (C) NIH-3T3 cells were treated overnight without (CRL) or with 2 mM of L-NAME in absence of serum. Then, cells were stimulated for 5, 10 and 20 min with serum, without (CRL) or with L-NAME. Representative Western blot images of p-ERK and total ERK. Tubulin was used as a loading control (D) Values are means ± SEM, n = 3 independent experiment. Relative ERK-phosphorylation levels were normalized to total protein and referred as a fold change of control. (E) α-SMA (green) expression in fat pad tumors is illustrated in paraffin tissue section with DAPI (blue). Scale bar: 5 μm.

MAP kinases signaling pathway has been suggested [41]. In addition, Switzer and col. demonstrated that S-Nitrosylation of EGFR activates a signaling pathway in human basal-like breast cancer [26]. Thus, we think that iNOS positive cells (ie LM3, LMM3 and MDA-MD-231) have evolved into an active mechanism associated with nitrosylation. We speculate that nitrosylation of MAPK signalling pathways take place in these cells. Although other post-translational modifications associated with NO cannot be ruled out. On the other hand, in cells that do not express the NOS enzymes, only the NO-independent mechanisms take place and therefore both the inhibition of NO production and its exogenous stimulation do not provide significant changes.

Several studies revealed that iNOS expression is associated with aggressive cancer and with worse prognosis in different types of tumor [4]. These results turn the enzymatic inhibition of iNOS as a promising

candidate to improve anticancer therapy [13]. In this sense, it has already been described that NOS inhibition suppresses tumor growth in breast, bladder and lung cancer models [10,14,29]. Using a bladder cancer model, we have previously revealed that L-NAME treatment was able to improve BCG-induced tumor inhibition. This bladder tumor reduction induced by L-NAME was associated with stroma activation [20,21]. According to our knowledge, how NO inhibition affects breast tumor stroma has been less addressed in research. To go further with this, the characteristic of the fibroblast-related stroma has been analyzed in mouse breast cancer models. Our result shows that L-NAME administration reduced tumor size together with activation of fibroblasts, showed as α-SMA expression, and collagen deposition only in iNOS positive tumors.

The administration of a NO donor, DETA/NO induced cytotoxicity in the NIH-3T3 fibroblasts line [30]. Furthermore, our results showed that NO inhibition increased proliferation of these fibroblasts. These results suggest that NO produced by cancer cells may inhibit the desmoplastic reaction by blocking proliferation and activation of fibroblasts. In this sense, it has been described that NO acts as a mediator regulating mitochondrial function. NO can activate a pro-tumoral fibroblast. In support of this notion, treatment with L-NAME was enough to reverse the pro-tumoral functions of associated fibroblast. (Ubaldo e [31].

There is information giving reference about the plasticity of the fibroblasts in the homeostasis of mammalian development. The resting fibroblasts serve as precursors of activated fibroblasts. The activated fibroblasts can differentiate in myofibroblasts, which can be involved in scar healing process, transform into fibroblasts synthetically active generating growth factors and extra cellular matrix, and also regulate tumor immunity and angiogenesis [32]. As a function of this plasticity, during the last years, several tumor fibroblast populations have been identified [18,33]. For example, one of four subsets, described by Costa et all, induced infiltration of immune suppressor regulatory T cells in breast tumors [33]. On the other hand, some evidence has been highlighted showing tumors with reduced desmoplasia accelerated tumor growth [34]. Therefore, we can assume that, depending on the status of the fibroblasts and the stage of tumor progression, that some of these populations behave either anti or pro tumoral [18]. Understanding the characteristics of activated fibroblasts population induced by L-NAME will contribute to the proposal to use pharmacological inhibitors as antitumor therapy.

In our syngenic model, inhibition of tumor growth induced by L-NAME is accompanied with activation of fibroblast. In vitro, L-NAME directly impacts on cancer cells and on fibroblast cells. It is also possible that L-NAME interferes in a dialogue in between both populations. In this sense, Martinez-Outschoorn and col, have demonstrated that NO over-production, secondary to Caveolin-1 loss, is the root cause for mitochondrial dysfunction in cancer associated fibroblasts. The treatment with L-NAME over co-culture of cancer cells and fibroblasts was enough) to abolish DNA double strand breaks on cancer cells [31]. These results suggest that L-NAME, reverses tumor cell mutations induced by protumoral fibroblasts. In other words, reduction of NO reverses the malignization of cancer cells induced by fibroblast. To deepen on this point, we have exposed LM3 or LMM3 cancer cells to the conditioned media collected from both NIH-3T3 or embryonic fibroblast treated or not with L-NAME. Conditioned media from L-NAME treated fibroblast did not modified LM3 or LMM3 cell viability. However, a reduction in the migratory capacity of LM3 cancer cells in contact with this conditioned media was observed (data not shown). This result suggests that NO inhibition could be affecting the secretion of soluble factors, which would affect cancer cells. Major efforts should be made to better understanding the dialogue between cancer and fibroblasts cells, particularly when NO is inhibited.

From the results presented and discussed here, we can assert that NO inhibition stimulates proliferation and activation of fibroblasts concurrently with the abrogation of iNOS-positive tumor cells growth. Hence, determination of iNOS expression in breast tumors and its pharmacological inhibition could be considered as new therapeutic targets to be added to conventional therapies.

4. Materials and methods

4.1. Cell culture

Murine hormone independent mammary cancer cell lines LM3, LMM3 [35] and LM2 [36] established in our Research Area were used. LM3 and LMM3 were maintained in MEM medium (Gibco). LM2 cell line was cultured in RPMI (Gibco). MDA-MB-231 were MCF10DCIS.com cell line was obtained from P. Chavrier's lab. and maintained in DMEM F12 supplemented with 2 mM L-glutamine, 80 μg/ml gentamycin and 5% horse serum (Gibco).

Fibroblasts NIH-3T3 (ATCC) cell line was maintained in DMEM low glucose (Gibco). All cultured media were supplemented with 2 mM L-glutamine, 80 μg/ml gentamycin and 5–10% fetal bovine serum (FBS) (Internegocios, Argentina) in a humidified atmosphere with 5% CO2 at 37 °C. Serial passages of confluent monolayers were performed by detaching cells with trypsin (0.25% trypsin and 0.075% EDTA in CA^{++} and Mg^{++} free PBS).

4.2. Cell viability assay

3×10^3 cells/100 μl were cultured in 96-well plates. After 24 h incubation, L-NAME (N L-NG-Nitroarginine Methyl Ester, Santa Cruz) (2 mM) or DETA/NO (250, 125 and 62 μM) was added and cells were cultured for 48 h or 24 h respectively. Cell viability was determined by the MTS assay (Promega).

4.3. NO production

NO production in tumor cell line supernatants was determined after 24 h either with or without the addition of L-NAME. Since NO is spontaneously transformed to nitrite, NO release was estimated as nitrite accumulation in the conditioned medium, compared to a sodium nitrite standard curve, using a modification of the Griess method [37].

4.4. Quantitative real time PCR

Total RNA from murine or human cell lines, were isolated with TRIZol Reagent (Invitrogen) as described [38]. Briefly, cDNA was synthesized using iScript-cDNA Synthesis-Kit (BioRad) and using as template for PCR and reactions were carried out in the CFX96 Real-Time System, C1000-Thermal-Cycler with TransStart Green qPCR SuperMix. Specific primers for mouse, iNOS Forward: 5′-TCAACACCAA GGTTGTCTGC-3′, Reverse: 5′-AAGGCCAAACACAGCATACC-3′, was normalized to GAPDH expression Forward: 5′-CAAAATGGTGAAGGTC GGTG-3′, Reverse: 5′-CAATGAAGGGG TCGTTGATG-3′. Human primers: iNOS Forward: 5′-ACAACAAATTCAGGTACGCTGTG-3; Reverse 5′-TCTGATCAATGTCATGAGCAAAGG-3 was normalized to GAPDH expression Forward: 5′-CAAAATGGTGAAGGTCGGTG-3′, Reverse: 5′-CAATGAAGGGGTCGTTGATG-3.

4.5. Western blot assay

Subconfluently monolayer of tumoral (LM3, LMM3, LM2, MDA-MB-231 or MCF10DCIS.com) or NIH-3T3 cells lines were treated with or without L-NAME 2 mM for 16 h without FBS. Then, cells were stimulated with 5% of FBS (with or without L-NAME) for 5, 10 and 20 min and processed for Western blot. Cells were gently washed with PBS and lysed using protein extraction lysis buffer (50 mM Tris-HCl (pH 8.0); 100 mM NaCl; 1% Triton, 1 mM/ml aprotinin, 1 mM phenylmethylsulfonyl fluoride, 2 mg/ml leupeptin and 10 mM EDTA/EGTA). Protein concentration was determined by Bradford method

according to the manufacturer's instruction (Merk). Aliquots from the cell lysates were separated by electrophoresis and analyzed in 10% sodium dodecyl sulfate-polyacrylamide gel (SDS-PAGE) and transferred onto a PVDF membrane. After blotting, the membrane was incubated with primary antibody p-ERK (sc-7383), iNOS (abcam, ab15323) nNOS (sc-5302), eNOS (sc-376751) and incubated with horseradish peroxidase conjugated secondary antibody (Sigma A9169; Millipore AP308P), for 1 h at room temperature. The blots were developed using the ECL detection kit and ImageQuant LAS 500 imager (GE Life sciences). Then, membranes were stripped and incubated over with ERK 1 (sc-93), tubulin (Ab 4074) or Beta-actin (Sigma, A5441), used as a loading control.

4.6. Immunofluorescence assay in culture cells

NIH-3T3 cells growing in chamber slides with complete medium were treated with L-NAME 2 mM. Sub confluent monolayers were gently washed in cold saline buffer and processed for immunofluorescence. Slides were fixed with PAF 4% in PBS for 15 min and permeabilized with Tritón X-100 0,3% Nonspecific antibody binding was blocked with a blocking solution containing 5% FBS plus Tween-20 0.1% in PBS for 60 min at room temperature. Fixed cells were incubated overnight with an antibody anti-α-SMA (Sigma). Rabbit IgG was used as isotype control. Goat anti-rabbit A488 (abcam, ab150077) or anti mouse A488 (abcam, ab150113) conjugate in PBS, served as the secondary antibody. Nuclei were counterstained with DAPI, slides were observed in a Nikon EclipseTM E400 fluorescence microscope and photographed with a CoolpixH 995 digital camera.

Histological and immunofluorescence of mouse tumor sections.

For immunofluorescence analysis on tissue sections, the following primary antibodies were used: iNOS (abcam, ab15323), E-cadherin (abcam, ab76055), anti-α-SMA (Sigma, A2547). Secondary antibodies anti-mouse IgG-Alexa488 (abcam, ab150113) and anti-rabbit- IgG-Alexa488 (abcam, ab150077) were used. To retrieve antigens on paraffin-embedded tissue samples, sections were incubated for 20 min in 10 mM sodium citrate buffer, pH 6.0 at 90 °C. Then, after 60-min incubation in 5% fetal calf serum, sections were incubated overnight with primary antibodies, washed and further incubated for 2 h at room temperature with appropriate secondary antibodies. Conventional Hematoxylin and Eosin staining was carried out and Masson's Trichrome (Biopack) and Picrosirious Red staining was performed according to manufacturer's instructions (NovaUltra, Woodstock, MD, USA). Quantification of collagen was analyzed using Image J software. Necrosis is defined as tissue area characterized by an increase in eosinophilia (hypereosinophilia) and homogeneous appearance, product of the denaturation of proteins; with phantom cellular figures by disintegration of cell membrane and pyknotic nuclei (of smaller size), with phenomena of caryolysis (rupture of nuclei), and karyorrhexis (nuclear fragmentation). Lymphocytes in H&E-stained sections were estimated according to the recommendations by the International TILs Working Group [39].

4.7. Fat pad tumor growth

Female BALB/c mice of 9 weeks old were inoculated in the fourth mammary gland with 2.5×10^5 LM3, LMM3 or LM2 cells. Then mice were randomized into 2 groups: Control and L-NAME (n = 8/group). Tumor growth was recorded twice weekly by measuring 2 perpendicular diameters. To calculate tumor size, the formula Volume = $3/4x\pi xDxd^2$ was used, where D and d represent the longer and shorter diameters, respectively. L-NAME (2 mM) was added to drinking water. The whole experiment was performed twice, obtaining the same result.

Ethics statement

BALB/c female mice (8 weeks old), were obtained from our Institute Animal Care Division.

Mice were handled in accordance with the international procedure for Care and Use of Laboratory Animals. Protocols were approved by the Institutional Review Board CICUAL, protocol number 2017/03, Institute of Oncology Angel H. Roffo.

Statistical analysis

All experiments were repeated three times independently. For MTS data is expressed as mean ± SD, n = 6; one representative experiment is showing. For WB quantification values correspond to means ± SEM, n = 3 independent experiment.

Student's *t*-test or Two-way ANOVA test and Bonferroni's contrast, employing Graph Pad InStat statistical package (version 6), was used. $p < 0.05$ was considered statistically significant.

Conflicts of interest

Authors declare no conflict of interest.

Aknowledgements

The authors greatly acknowledge the Animal facility from Instituto de Oncología Angel H. Roffo. M.S. is supported by Instituto Nacional del Cancer. M. Z is supported by Universidad de Buenos Aires. This work was supported by Consejo Nacional de Investigaciones Científicas y Tecnológicas (CONICET) PIP 2015–2017 and Universidad de Buenos Aires UBACyT 2016. We are grateful to Inés Kletzky for revising our English version.

References

[1] J. Ferlay, I. Soerjomataram, R. Dikshit, S. Eser, C. Mathers, M. Rebelo, ... F. Bray, Cancer incidence and mortality worldwide: sources, methods and major patterns in GLOBOCAN 2012, Int. J. Cancer 136 (5) (2015) E359–386, https://doi.org/10.1002/ijc.29210.

[2] C.M. Perou, T. Sorlie, M.B. Eisen, M. van de Rijn, S.S. Jeffrey, C.A. Rees, ... D. Botstein, Molecular portraits of human breast tumours, Nature 406 (6797) (2000) 747–752, https://doi.org/10.1038/35021093.

[3] R.G. Knowles, S. Moncada, Nitric oxide synthases in mammals, Biochem. J. 298 (Pt 2) (1994) 249–258.

[4] D. Basudhar, S.A. Glynn, M. Greer, V. Somasundaram, J.H. No, D.A. Scheiblin, ... D.A. Wink, Coexpression of NOS2 and COX2 accelerates tumor growth and reduces survival in estrogen receptor-negative breast cancer, Proc. Natl. Acad. Sci. U. S. A. 114 (49) (2017) 13030–13035, https://doi.org/10.1073/pnas.1709119114.

[5] J.R. Hickok, D.D. Thomas, Nitric oxide and cancer therapy: the emperor has NO clothes, Curr. Pharmaceut. Des. 16 (4) (2010) 381–391.

[6] A.J. Burke, F.J. Sullivan, F.J. Giles, S.A. Glynn, The yin and yang of nitric oxide in cancer progression, Carcinogenesis 34 (3) (2013) 503–512, https://doi.org/10.1093/carcin/bgt034.

[7] W. Zhang, X.J. He, Y.Y. Ma, H.J. Wang, Y.J. Xia, Z.S. Zhao, ... H.Q. Tao, Inducible nitric oxide synthase expression correlates with angiogenesis, lymphangiogenesis, and poor prognosis in gastric cancer patients, Hum. Pathol. 42 (9) (2011) 1275–1282, https://doi.org/10.1016/j.humpath.2010.09.020.

[8] E.O. Sandes, A.G. Faletti, M.D. Riveros, C. Vidal Mdel, L. Gimenez, A.R. Casabe, A.M. Eijan, Expression of inducible nitric oxide synthase in tumoral and non-tumoral epithelia from bladder cancer patients, Nitric Oxide 12 (1) (2005) 39–45, https://doi.org/10.1016/j.niox.2004.11.003.

[9] L. Yang, Y. Wang, L. Guo, L. Wang, W. Chen, B. Shi, The expression and correlation of iNOS and p53 in oral squamous cell carcinoma, BioMed Res. Int. 2015 (2015) 637853, https://doi.org/10.1155/2015/637853.

[10] D. Belgorosky, Y. Langle, B. Prack Mc Cormick, L. Colombo, E. Sandes, A.M. Eijan, Inhibition of nitric oxide is a good therapeutic target for bladder tumors that express iNOS, Nitric Oxide 36 (2014) 11–18, https://doi.org/10.1016/j.niox.2013.10.010.

[11] S. Granados-Principal, Y. Liu, M.L. Guevara, E. Blanco, D.S. Choi, W. Qian, ... J.C. Chang, Inhibition of iNOS as a novel effective targeted therapy against triple-negative breast cancer, Breast Cancer Res. 17 (2015) 25, https://doi.org/10.1186/s13058-015-0527-x.

[12] P. Garrido, A. Shalaby, E.M. Walsh, N. Keane, M. Webber, M.M. Keane, ... S.A. Glynn, Impact of inducible nitric oxide synthase (iNOS) expression on triple negative breast cancer outcome and activation of EGFR and ERK signaling pathways, Oncotarget 8 (46) (2017) 80568–80588, https://doi.org/10.18632/oncotarget.19631.

[13] S.A. Glynn, B.J. Boersma, T.H. Dorsey, M. Yi, H.G. Yfantis, L.A. Ridnour, ... S. Ambs, Increased NOS2 predicts poor survival in estrogen receptor-negative breast cancer

patients, J. Clin. Investig. 120 (11) (2010) 3843–3854, https://doi.org/10.1172/JCI42059.
[14] J.L. Heinecke, L.A. Ridnour, R.Y. Cheng, C.H. Switzer, M.M. Lizardo, C. Khanna, ... D.A. Wink, Tumor microenvironment-based feed-forward regulation of NOS2 in breast cancer progression, Proc. Natl. Acad. Sci. U. S. A. 111 (17) (2014) 6323–6328, https://doi.org/10.1073/pnas.1401799111.
[15] N. Bettaga, R. Jager, S. Dunnes, D. Groneberg, A. Friebe, Cell-specific impact of nitric oxide-dependent guanylyl cyclase on arteriogenesis and angiogenesis in mice, Angiogenesis 18 (3) (2015) 245–254, https://doi.org/10.1007/s10456-015-9463-8.
[16] A. Ocana, C. Nieto-Jimenez, A. Pandiella, A.J. Templeton, Neutrophils in cancer: prognostic role and therapeutic strategies, Mol. *Cancer* 16 (1) (2017) 137, https://doi.org/10.1186/s12943-017-0707-7.
[17] M.A. Rahat, B. Hemmerlein, Macrophage-tumor cell interactions regulate the function of nitric oxide, Front. Physiol. 4 (2013) 144, https://doi.org/10.3389/fphys.2013.00144.
[18] R. Kalluri, The biology and function of fibroblasts in cancer, Nat. Rev. Cancer 16 (9) (2016) 582–598, https://doi.org/10.1038/nrc.2016.73.
[19] M.W. Conklin, J.C. Eickhoff, K.M. Riching, C.A. Pehlke, K.W. Eliceiri, P.P. Provenzano, ... P.J. Keely, Aligned collagen is a prognostic signature for survival in human breast carcinoma, Am. J. Pathol. 178 (3) (2011) 1221–1232, https://doi.org/10.1016/j.ajpath.2010.11.076.
[20] V. Alvarez, C. Lodillinsky, S. Umerez, E. Sandes, A.M. Eijan, Inhibition of bacillus Calmette-Guerin-induced nitric oxide in bladder tumor cells may improve BCG treatment, Int. J. Mol. Med. 16 (4) (2005) 565–571.
[21] C. Lodillinsky, Y. Langle, A. Guionet, A. Gongora, A. Baldi, E.O. Sandes, ... A.M. Eijan, Bacillus Calmette Guerin induces fibroblast activation both directly and through macrophages in a mouse bladder cancer model, PLoS One 5 (10) (2010) e13571, , https://doi.org/10.1371/journal.pone.0013571.
[22] B.C. Ozdemir, T. Pentcheva-Hoang, J.L. Carstens, X. Zheng, C.C. Wu, T.R. Simpson, ... R. Kalluri, Depletion of carcinoma-associated fibroblasts and fibrosis induces immunosuppression and accelerates pancreas cancer with reduced survival, Cancer Cell 28 (6) (2015) 831–833, https://doi.org/10.1016/j.ccell.2015.11.002.
[23] L. Rossi, D. Stevens, J.Y. Pierga, F. Lerebours, F. Reyal, M. Robain, ... R. Rouzier, Impact of adjuvant chemotherapy on breast cancer survival: a real-World population, PLoS One 10 (7) (2015) e0132853, , https://doi.org/10.1371/journal.pone.0132853.
[24] C. Global Burden of Disease Cancer, C. Fitzmaurice, C. Allen, R.M. Barber, L. Barregard, Z.A. Bhutta, ... M. Naghavi, Global, regional, and national cancer incidence, mortality, years of Life lost, years lived with disability, and disability-adjusted life-years for 32 cancer groups, 1990 to 2015: a systematic analysis for the global burden of disease study, JAMA Oncol 3 (4) (2017) 524–548, https://doi.org/10.1001/jamaoncol.2016.5688.
[25] D.D. Browning, M.P. McShane, C. Marty, R.D. Ye, Nitric oxide activation of p38 mitogen-activated protein kinase in 293T fibroblasts requires cGMP-dependent protein kinase, J. Biol. Chem. 275 (4) (2000) 2811–2816.
[26] C.H. Switzer, S.A. Glynn, R.Y. Cheng, L.A. Ridnour, J.E. Green, S. Ambs, D.A. Wink, S-nitrosylation of EGFR and Src activates an oncogenic signaling network in human basal-like breast cancer, Mol. Cancer Res. 10 (9) (2012) 1203–1215, https://doi.org/10.1158/1541-7786.MCR-12-0124 Epub 2012 Aug 9.
[27] H.P. Monteiro, E.G. Rodrigues, A.K.C. Amorim Reis, L.S. Longo Jr., F.T. Ogata, A.I.S. Moretti, P.E. da Costa, A.C.S. Teodoro, M.S. Toledo, S. M, A. Stern, Nitric oxide and interactions with reactive oxygen species in the development of melanoma, breast, and colon cancer: a redox signaling perspective, Nitric Oxide 10 (2019) 1016/j.niox.2019.04.009.
[28] L.A. Ridnour, K.M. Barasch, A.N. Windhausen, T.H. Dorsey, M.M. Lizardo, H.G. Yfantis, D.H. Lee, C.H. Switzer, R.Y. Cheng, J.L. Heinecke, E. Brueggemann, H.B. Hines, C. Khanna, S.A. Glynn, S. Ambs, D.A. Wink, Nitric oxide synthase and breast cancer: role of TIMP-1 in NO-mediated Akt activation, PLoS One 7 (9) (2012) e44081, , https://doi.org/10.1371/journal.pone.0044081 Epub *2012 Sep 5. doi:10.1073/pnas.0502979102*.
[29] N.L. Pershing, C.F.J. Yang, M. Xu, C.M. Counter, Treatment with the nitric oxide synthase inhibitor L-NAME provides a survival advantage in a mouse model of Kras mutation-positive, non-small cell lung cancer, Oncotarget 7 (27) (2016) 42385–42392, https://doi.org/10.18632/oncotarget.9874.
[30] L.S. Bittencourt, D.C. Machado, M.M. Machado, G.F. Dos Santos, T.D. Algarve, D.R. Marinowic, ... I.B. Cruz, The protective effects of guarana extract (Paullinia cupana) on fibroblast NIH-3T3 cells exposed to sodium nitroprusside, Food Chem. Toxicol. 53 (2013) 119–125, https://doi.org/10.1016/j.fct.2012.11.041.
[31] U.E. Martinez-Outschoorn, R.M. Balliet, D.B. Rivadeneira, B. Chiavarina, S. Pavlides, C. Wang, D. Whitaker-Menezes, K.M. Daumer, Z. Lin, A.K. Witkiewicz, N. Flomenberg, A. Howell, R.G. Pestell, E.S. Knudsen, F. Sotgia, M.P. Lisanti, Oxidative stress in cancer associated fibroblasts drives tumor-stroma co-evolution: a new paradigm for understanding tumor metabolism, the field effect and genomic instability in cancer cells, Cell Cycle. 2010 Aug 15 9 (16) (2010) 3256–3276, https://doi.org/10.4161/cc.9.16.12553 Epub 2010 Aug 28.
[32] M. Zeisberg, F. Strutz, G.A. Muller, Role of fibroblast activation in inducing interstitial fibrosis, J. Nephrol. 13 (Suppl 3) (2000) S111–120.
[33] A. Costa, Y. Kieffer, A. Scholer-Dahirel, F. Pelon, B. Bourachot, M. Cardon, ... F. Mechta-Grigoriou, Fibroblast heterogeneity and immunosuppressive environment in human breast cancer, Cancer Cell 33 (3) (2018) 463–479, https://doi.org/10.1016/j.ccell.2018.01.011 e410.
[34] A.D. Rhim, P.E. Oberstein, D.H. Thomas, E.T. Mirek, C.F. Palermo, S.A. Sastra, ... B.Z. Stanger, Stromal elements act to restrain, rather than support, pancreatic ductal adenocarcinoma, Cancer Cell 25 (6) (2014) 735–747, https://doi.org/10.1016/j.ccr.2014.04.021.
[35] A. Urtreger, V. Ladeda, L. Puricelli, A. Rivelli, M. Vidal, E. Delustig, E. Joffe, Modulation of fibronectin expression and proteolytic activity associated with the invasive and metastatic phenotype in two new murine mammary tumor cell lines, Int. J. Oncol. 11 (3) (1997) 489–496.
[36] S. Galli, L. Colombo, S. Vanzuli, M.C. Daroqui, M. del Carmen Vidal, M.A. Jasnis, ... A.M. Eijan, Characterization of a fibroblastoid mammary carcinoma cell line (LM2) originated from a mouse adenocarcinoma, Int. J. Oncol. 17 (6) (2000) 1259–1265.
[37] J. Xu, X. Xu, W. Verstraete, Adaptation of E. coli cell method for micro-scale nitrate measurement with the Griess reaction in culture media, J. Microbiol. Methods 41 (1) (2000) 23–33.
[38] Y.V. Langle, D. Belgorosky, B. Prack McCormick, A. Sahores, A. Góngora, A. Baldi, C. Lanari, C. Lamb, A.M. Eiján, FGFR3 down-regulation is involved in bacillus calmette-guérin induced bladder tumor growth inhibition, J Urol. 195 (1) (2016) 188–197, https://doi.org/10.1016/j.juro.2015.06.093 Epub 2015 Jul 2.
[39] R. Salgado, C. Denkert, S. Demaria, et al., The evaluation of tumor-infiltrating lymphocytes (TILs) in breast cancer: recommendations by an International TILs Working Group 2014, Ann. Oncol. 26 (2) (2015) 259–271, https://doi.org/10.1093/annonc/mdu450.
[40] D. Basudhar, V. Somasundaram, G.A. de Oliveira, A. Kesarwala, J.L. Heinecke, R.Y. Cheng, ... L.A. Ridnour, Nitric oxide synthase-2-derived nitric oxide drives multiple pathways of breast cancer progression, Antioxidants Redox Signal. 26 (18) (2017) 1044–1058, https://doi.org/10.1089/ars.2016.6813.
[41] C.J. Oliveira, F. Schindler, A.M. Ventura, M.S. Morais, R.J. Arai, V. Debbas, A. Stern, H.P. Monteiro, Nitric oxide and cGMP activate the Ras-MAP kinase pathway-stimulating protein tyrosine phosphorylation in rabbit aortic endothelial cells, Free Radic. Biol. Med. 35 (2003) 381–396, https://doi.org/10.1016/s0891-5849(03)00311-3.